ELSEVIER

Chemical Engineering Science 62 (2007) 4579–4588

Chemical Engineering Science

www.elsevier.com/locate/ces

Micro-oxygenation of wine in presence of dissolved carbon dioxide

Audrey Devatine*, Igor Chiciuc, Christian Poupot, Martine Mietton-Peuchot

University Bordeaux 2, Facutly of Enology, 351 Cours de la Libération, 33405 Talence Cedex, France

Received 30 January 2007; received in revised form 30 April 2007; accepted 23 May 2007
Available online 29 May 2007

Abstract

Techniques for micro-oxygenation of wines are now accepted practices in wine manufacturing. But, at present time, only wine tasting and empirical know-how are used to control the oxygen input. Our work aims at a better control of oxygen input in wine, where oxygen plays a role through its solubilization and its consumption by various substrates in the wine. This work aims at implementing concepts from conventional chemical engineering, i.e., mass transfer between two fluid phases, to rationalize, quantify and master the oxygen input during or just after vinification, in respect to the quantities demanded by the wine processing. In particular, the work presented here concerns the incidence of dissolved carbon dioxide in wine on oxygen transfer. This parameter must be considered when the micro-oxygenation is applied during or after alcoholic fermentation. This study shows that the presence of dissolved carbon dioxide affects strongly the efficiency of the transfer of oxygen to the liquid: it almost decreases one order of magnitude when carbon dioxide concentration changes from 0 to 1.4 g/L. For convenience and reproducibility, experiments were performed on synthetic solutions, but part of the results was validated on real wine. An explanation based on a simplified physical description is proposed.

Keywords: Absorption; Aeration; Bubble columns; Mass transfer; Micro-oxygenation; Wine

1. Introduction

All along vinification and ageing, as well as during ageing of the bottled wine, oxygen is a major actor in the wine transformation. It has a beneficial role in many steps of the wine making process (increase of the yeast population, colour stabilization, etc.), but oxygen may also be detrimental when present during specific steps (oxidation, growth of micro-organisms, etc.).

Solubilization of oxygen into broths or wines occurs when gaseous oxygen is brought into contact with the liquid. This is on purpose, as when aerated withdrawals are operated, (where oxygen concentration from 3 mg/L up to saturation can be obtained, (Moutounet and Mazauric, 2001)), or when hyper-oxygenation or micro-oxygenation are operated. This may also be an unavoidable side effect of filtration, cooling or bottling operations (Castellari et al., 2004).

Oxygen of the surrounding air may easily dissolve into grape broths and wines. But, in contrast with nitrogen or carbon dioxide, oxygen, when dissolved, is quickly consumed, as it is involved in numerous mechanisms of oxydo-reduction reactions. Phenolic components from the grape are the main consumers of oxygen (around 60%) (Fabre, 1994). Therefore, red wines exhibit faster consumption kinetics than white wines (Moutounet and Mazauric, 2001). Other components may be involved in this consumption, like ethanol (around 20%), resulting in the formation of ethanal, and sulfur dioxide (around 12%).

Oxygen input to wine, and therefore its consumption, may vary all along the vinification. White wine broths are very oxidation sensitive, because of their low antioxidant content. To insure better stability for these wines, hyper-oxygenation, a technique using vigorous oxygen bubbling, is operated to induce browning reactions due to polyphenol oxidation (Getaz and Fabre, 1990; Schneider, 1991, 1998). The consequences of this technique upon the vinification process, used only on white broths, has been described (Artajona et al., 1990; Blanck, 1990; Dubourdieu and Lavigne, 1990; Meistermann, 1990).

During alcoholic fermentation, oxygen input improves fermentation kinetics and decreases the risks for fermentation failure, by increasing cell viability at the end of the fermentation

* Corresponding author.
E-mail address: audrey.devatine@oenologie.u-bordeaux2.fr (A. Devatine).

0009-2509/$ - see front matter © 2007 Elsevier Ltd. All rights reserved.
doi:10.1016/j.ces.2007.05.031

(Strehaiano, 1990; Sablayrolles, 1990; Lafon Lafourcade and Larue, 1981).

During maturing of the wine, oxygen input may have a structuring effect, namely by favouring colour stabilization, degradation of vegetal characteristics and disappearance of reduction taste. Traditionally, wine breeding is conducted inside barrels, and measurement of dissolved oxygen usually shows that oxygen concentration remains always very low ($< 50\,\mu g/L$). Indeed, oxygen is consumed faster than it is provided because the maturing in barrels corresponds to a slow and continuous dissolution of oxygen due to permanent oxygen diffusion through the wood barrel walls and technological inputs (racking, topping-up, etc.). But quantification and control of oxygen input during these conventional maturation processes have never been controlled.

Considering ageing of the wine inside bottles, Lopes et al. (2005) have evidenced different diffusive oxygen inputs through the bottle stopper, depending upon the kind of stopper used.

So, the principle of a micro-oxygenation technique is to incorporate continuously small controlled oxygen amounts into the wine, stored inside tanks. As for barrel wine breeding, these amounts must be always inferior to the instantaneous consumption, in order to prevent from any accumulation of oxygen (Moutounet et al., 1995).

So, it is obvious that, for the wine maker, the ability to control the oxygen input in the broth would be a great help to master the vinification process. Ageing in barrels is mainly done because this technique delivers the adapted oxygen flux for the maturation process. But this technique is not convenient and not cost effective, and ageing in large tanks is without any doubt more adapted to large productions, provided the same quality is obtained. Up to now the most used micro-oxygenation technique consists in generating microbubbles of pure gaseous oxygen in the wine tank using a porous gas distributor. Oxygen perfusion through membranes, as used in animal cell culture, was never proposed. The microbubbling technique is now the accepted practice in wine manufacturing. But, up to now, the oxygen input is only monitored by tasting, and no rational technical analysis of the transfer efficiency of this process has been done. Implementation of chemical engineering concepts to these oxygenation techniques, to obtain modelling of the mass transfer phenomena between the gaseous oxygen and the liquid phase, should allow better understanding. So, scientific rules to master the technique could be proposed.

Many works in chemical engineering literature have been devoted to oxygenation techniques, especially concerning fermentation processes, but very few have specifically addressed their application to the wine process. Indeed, influence upon the transfer of oxygen, of the specific superficial tension of the wine, due to the tensio-active properties of certain of its constituents, has been pointed out (Painmanakul et al., 2005). Farines et al. (2005) have studied the oxygen transfer in wine, and have characterized the oxygen transfer using the conventional K_La parameter, the volumetric mass transfer coefficient, which does not dissociate transfer area and diffusional resistance. In this first approach, using synthetic solutions, Farines et al. (2005) identified prominent parameters influencing this transfer coefficient, taking into account the ethanol concentration and the sugar concentration. In particular, they pointed out the surprising dramatic influence of the dissolved carbon dioxide. Indeed, when the liquid was carbon dioxide saturated, a strong decrease of K_La values was observed, and no satisfying explanation was proposed. The works presented here address this issue, and especially attempt to a better understanding of the incidence of dissolved carbon dioxide in wine upon oxygen transfer. Indeed, during or after alcoholic fermentation, high concentrations of carbon dioxide, up to saturation (1.4 g/L at 20 °C), are present in the liquid, and this parameter must be considered when the micro-oxygenation is applied. The study will first present a preliminary set of experiments, performed in a 3 L agitated reactor and in a bubble column, and are devoted to validate the methods, experimental as well as mathematical, to obtain values of K_La on the experimental device. This latter was chosen to be representative of the actual micro-oxygenation operation in large tanks. Indeed, gentle bubbling in an immobile liquid phase in a column (4 or 20 L, either filled with a synthetic solution, or real wine), using specific porous distributors used for micro-oxygenation, was considered to achieve this goal. Even imperfect, this situation allows analysis of K_La values for further understanding of the phenomenon, especially concerning the influence of carbon dioxide. For convenience and reproducibility, the experiments were performed on synthetic solutions, but part of the results was validated for real wine oxygenation.

2. Material and methods

2.1. Experimental setup

Preliminary tests to validate the method were done using a 3 L glass tank stirred at 700 rpm, where gas is injected at the bottom via a high density polyethylene distributor (Porex) with pore mean diameter between 7 and 12 μm. Every run is done with 2.5 L of solution.

For the study itself, as mentioned in the introduction, a bubble column (height: 2.5 m, diameter: 0.1 m) was used, where gas injection is done at the bottom using ceramic type porous distributors, specifically designed for micro-oxygenation. The experimental apparatus is shown in Fig. 1.

Two kinds of distributors were tested: a cylindrical distributor (Enodev) with a mean pore diameter of 2 μm and a plate distributor (Parsec) with a mean pore diameter of 3.5 μm. Previous works in the laboratory have shown very similar performance, in terms of transfer, for these two devices. With this column, experiments were performed using two configurations: 4 or 20 L of liquid.

In all experiments, gases (nitrogen, synthetic air, pure oxygen or carbon dioxide) come from pressurized bottles and, in all cases, their flow rate was set to 0.05 L/min, at Normal Conditions. Synthetic air is composed of 20% oxygen and 80% nitrogen.

The synthetic solution is a hydroalcoholic mixture (12% volumic) containing 5 g/L tartric acid (pH = 3.5) and different

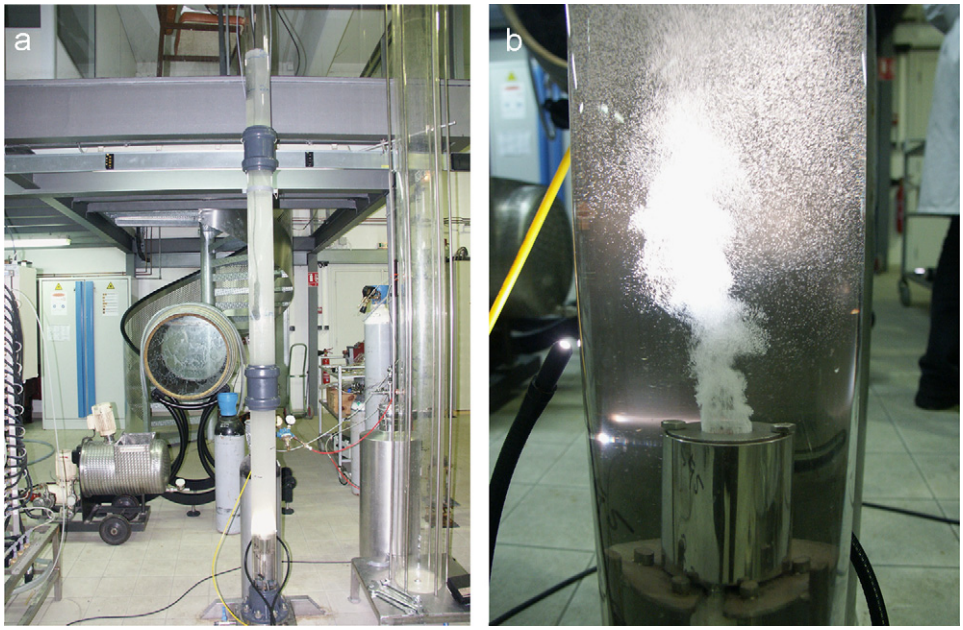

Fig. 1. (a) General view of the experimental bubble column. (b) Detailed view of the ceramic gas distributor.

concentrations of dissolved carbon dioxide (from 0 to 1.4 g/L). Experiments with a real wine, were done using a red wine with the following characteristics: 12% v/v ethanol, pH = 3.5, total acidity = 5.1 g/L of tartaric acid and two concentrations of dissolved CO_2 (0 and 1.4 g/L).

For all experiments, except those of Section 3.1.3, oxygen concentration was measured using an LDO optical oxygen probe (0.01–20 mg/L; Hach Lange). Indeed, our experiments require a probe with low response time in order to make a correct determination of K_La. The optical probe fulfils this requirement with a response time of around 5 s, while the polarographic probe (Cellox 325 (20–50 mg/L; WTW) exhibits a 90 s response time. When performing saturation with pure oxygen, the limited range of the optical probe (20 mg/L) does not allow obtaining the complete curve (up to 41 mg/L), but this drawback was judged negligible. It was also noted that accumulation of rising gas bubbles was likely to influence the measurement; therefore, the probe was set in an inverse position, i.e., its head directed upwards. The oxygen probe is located at 0.37 or 2 m from the bottom of the column, depending on the volume of solution in the column (4 or 20 L). In Section 3.1.3, for comparison of absorption experiments with air or pure oxygen, the polarographic probe was used.

Carbon dioxide concentration is obtained from discrete chemical assays using a conventional method (Caputi et al., 1970).

2.2. Methods

Volumetric transfer coefficient is obtained from a conventional dynamic method: first, oxygen is desorbed by nitrogen injection, and when the oxygen probe indicates zero oxygen concentration, nitrogen is replaced by synthetic air or pure oxygen, at the same flow rate. The oxygen concentration increase is then recorded. This kind of experiment is termed "absorption experiment". From the conventional model, that assumes homogeneous concentration in the vessel and constant saturation concentration, C^*, in time and space, K_La is obtained from the slope of the curve:

$$\ln\frac{C^*-C_i}{C^*-C}=K_Lat, \tag{1}$$

where C_i is the initial oxygen concentration (0 in this case), and C, the instantaneous oxygen concentration.

This method can be extended to "desorption experiments", where nitrogen is injected to strip dissolved oxygen from a saturated solution, and where decrease of the initial oxygen concentration is recorded. This method is claimed to be more accurate (Wild et al., 1994), because knowledge of C^* is not needed (this feature proved to be useful when interpreting results upon the influence of dissolved carbon dioxide). In this case, K_La values are here obtained from the equation:

$$\ln\frac{C_i}{C}=K_Lat. \tag{2}$$

The estimation of the transfer efficiency can be quantified by the value of the oxygen transfer yield Y, defined as the ratio of the maximum transferable oxygen flux, $K_LaC^*V_c$, to the oxygen flux entering via the gas flow, $D(P_{O_2}/P_T)(1/V_{mol})M_{O_2}$. Introducing Henry's constant, from Henry's law, written as $P_{O_2}=HC^*$, it is obtained:

$$Y=\frac{K_LaV_cP_TV_{mol}}{DM_{O_2}H}. \tag{3}$$

It is important to describe in detail the procedure to obtain oxygen absorption and desorption curves in presence of CO_2.

First, all dissolved gases are desorbed by nitrogen injection. Then, the column is carbon dioxide saturated by injecting pure CO_2, and final CO_2 concentration is assayed. Pure oxygen or synthetic air is injected, and recording of the increase of the oxygen concentration by the LDO probe (up to 20 mg/L, which is the maximum range of the probe), provides the absorption curve. When oxygen concentration has reached the value 20 mg/L, gas injection is stopped and carbon dioxide is then assayed; its concentration has dropped because of its concomitant desorption during the previous oxygen loading. Then nitrogen is injected, and recording of the decrease of oxygen concentration by the LDO probe provides the desorption curve, referred to an initial CO_2 concentration corresponding to the previous assay. By essence, this procedure does not allow to obtain a desorption curve referred to a saturated carbon dioxide concentration, because oxygen loading will inevitably desaturate the solution, in respect to carbon dioxide.

3. Results and discussion

3.1. Preliminary validation tests

3.1.1. Evaluation of the oxygen saturation concentration

The value of the saturation concentration for oxygen C^* in a given liquid is a key parameter for the determination of K_La using absorption experiments. Indeed this value is involved in the evaluation of the potential of transfer $(C^* - C)$. For a given temperature, C^* depends on the nature of the liquid and its dependence upon the partial pressure of oxygen in the gas is given by Henry's law, $P_{O_2} = HC^*$. To insure better accuracy, instead of using values of Henry's constant from the literature, specific experiments were performed to determine its value, for our synthetic solution and the wine. So, saturation experiments were performed with ambient air (from a compressor, partial pressure of oxygen 0.2095 atm), and equilibrium oxygen concentration is measured in the liquid (LDO probe) after sufficient time to insure equilibrium between gas and liquid in the agitated 1L becher.

So, at ambient temperature, 19 °C, the experimental values obtained for the Henry's constant are then $H = 2.47$ MPa L/g for the synthetic solution, and $H = 2.72$ MPa L/g for the wine. From these results, computed values of the saturation concentration of the synthetic solution, with synthetic air and pure oxygen are then $C^* = 8.2$ and 41.1 mg/L, respectively. For wine, computed values of the saturation concentration for synthetic air and pure oxygen are then $C^* = 7.4$ and 37.2 mg/L, respectively.

3.1.2. Comparison of K_La values obtained from absorption or desorption experiments

In Fig. 2a is shown an example of dissolved oxygen concentration curves for an absorption experiment (with synthetic air, increasing curve) and a desorption experiment (with nitrogen, decreasing curve). Fig. 2b presents the mathematical processing of the data to obtain K_La from the slopes of the curves. Note that for desorption experiment C^* is taken as 0 in the equation. As expected, it is shown that K_La values from desorption experiments or absorption experiments are very similar (around 5×10^{-3} s^{-1}) and this result validates the method.

Same type of experiments were done in the 4 L column, using pure oxygen. Figs. 3a and b show that, in this case also, K_La values are similar (3.69×10^{-3} and 4.09×10^{-3} s^{-1}).

Same type of experiments were also done in the 20 L column, using synthetic air, and similar values for K_La are also found (1.26×10^{-3} and 1.58×10^{-3} s^{-1}, for absorption and desorption respectively, see Figs. 4a and b).

In both cases (4 and 20 L column), it can be suspected here that absorption K_La values suffer from the inaccuracy upon C^*, that is not constant in the column, due to the hydrostatic pressure. Conversely desorption experiments are not affected by this hypothesis of spatial constancy of C^*, because C^* is not involved in the calculation (Eq. (2)). Another explanation may also lie in a deviation for the hypothesis of perfectly mixed liquid phase. At this point, the accuracy of the conventional method of determination of K_La, for this configuration, i.e., the bubble column, may be discussed.

3.1.3. Comparison of K_La values obtained from absorption experiments with air or pure oxygen

hboxFig. 5b presents the processed curve for an absorption experiment with pure oxygen, using a polarographic probe in the 3 L agitated reactor, where K_La is determined equal to $K_La = 5.24 \times 10^{-3}$ s^{-1}. This value compares with similar experiments of Fig. 2 where synthetic air was used, and where $K_La = 4.82 \times 10^{-3}$ s^{-1} was obtained. Note that for experiment of Fig. 5a, oxygen concentration was measured using the polarographic probe, whose response time is not very small in respect to the duration of the experiment. Indeed, for this experiment, K_La is obtained from the last points of the curve of Fig. 5a (after 100 s) where concentration evolution is slowed enough to be compatible with the low dynamics of the probe. Anyway, these experiments confirm, as expected, that the mass transfer conductance K_La, is not dependent on the oxygen partial pressure in the gaseous stream. Nevertheless, note that using pure oxygen obviously achieves higher transferred fluxes.

3.2. Influence of the dissolved carbon dioxide concentration upon oxygen transfer

3.2.1. Oxygen absorption and desorption in presence of dissolved carbon dioxide

The tests are at first done in the 4 L column and Fig. 6a presents the influence of initial dissolved carbon dioxide concentration upon the values of K_La, when injection of pure oxygen in the synthetic solution is done. These values are determined either from absorption (▲ curve) or desorption (● curve) experiments, using the model described above, where it is reminded that saturation concentration C^* is assumed to be constant in time and space. Values of K_La, for absorption experiments, show a strong decrease when initial carbon dioxide concentration is increased. Conversely, and very surprisingly, the opposite variation occurs for desorption experiments.

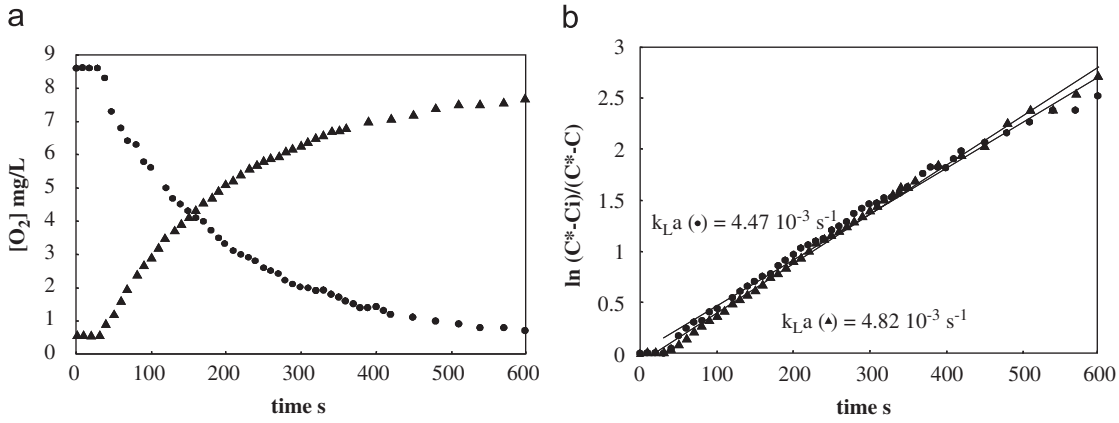

Fig. 2. (a) Absorption curve (▲) and desorption curve (•) obtained in a 3 L reactor—Porex distributor—synthetic solution—with synthetic air and nitrogen ($D = 0.05$ L/ min). (b) Determination of $K_L a$ for absorption curve (▲) and desorption curve (•). Conditions as for Fig. 2a.

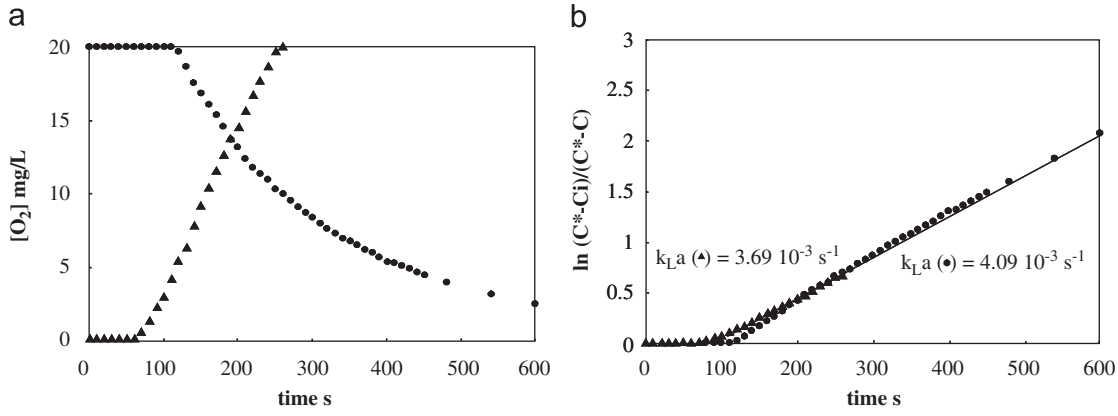

Fig. 3. (a) Absorption curve (▲) and desorption curve (•) obtained in a 4 L column—Parsec distributor—synthetic solution—with pure oxygen and nitrogen ($D = 0.05$ L/ min). (b) Determination of $K_L a$ for absorption curve (▲) and desorption curve (•). Conditions as for Fig. 3a.

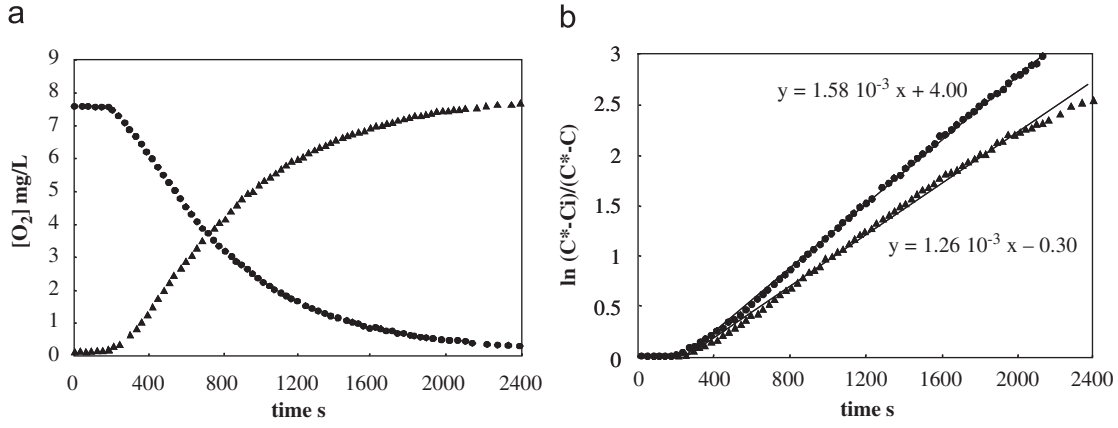

Fig. 4. (a) Absorption curve (▲) and desorption curve (•) obtained in a 20 L column—Œnodev distributor—synthetic solution—with synthetic air and nitrogen ($D = 0.05$ L/min). (b) Determination of $K_L a$ for absorption curve (▲) and desorption curve (•). Conditions as for Fig. 4a.

Fig. 6b presents the computed values of the oxygen transfer yield for absorption, where it is seen the correlative loss of oxygen transfer efficiency when carbon dioxide is present.

Using the 20 L column, with injection of synthetic air in a synthetic solution, similar results were found (Fig. 7a) and same variation of $K_L a$ values is observed, depending on the direction of transfer, i.e., absorption or desorption. Fig. 7b presents the same decrease of the absorption transfer yields, which proved to be nevertheless higher than for the 4 L column (almost 100% for carbon dioxide free solution). This is probably due to the longer residence time of the gas bubbles in the column.

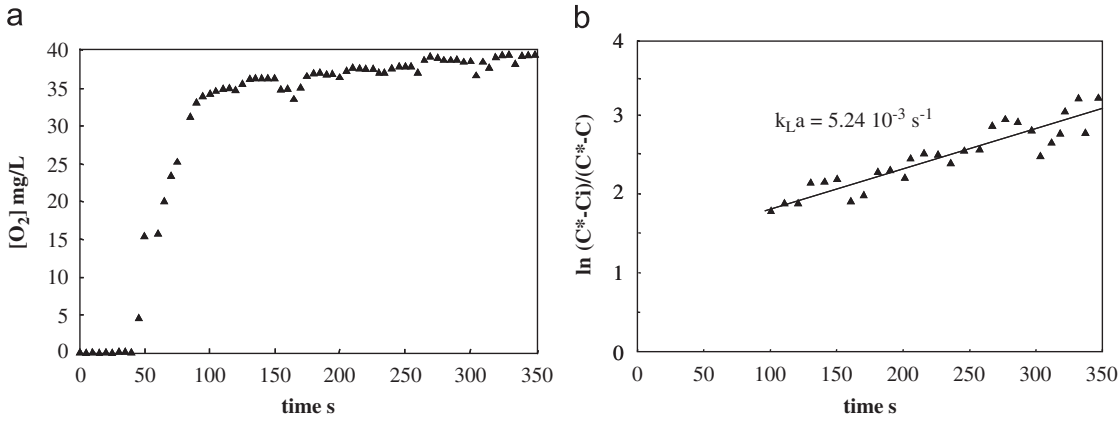

Fig. 5. (a) Absorption curve obtained in a 3 L reactor—Porex distributor—synthetic solution—with pure oxygen and nitrogen (D=0.05 L/min). (b) Determination of K_La for absorption curve. Conditions as for Fig. 5a.

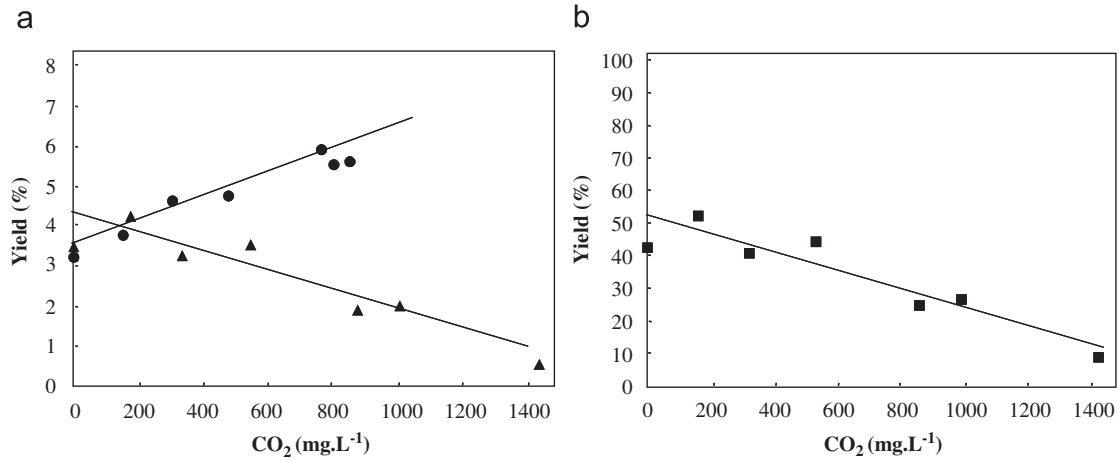

Fig. 6. (a) Values of K_La versus initial CO_2 concentration for absorption experiments (▲) and for desorption experiments (●) in a 4 L column—Parsec distributor—synthetic solution—with pure oxygen and nitrogen (D = 0.05 L/min). (b) Oxygen transfer yield for different initial CO_2 concentrations. Conditions as for Fig. 6a.

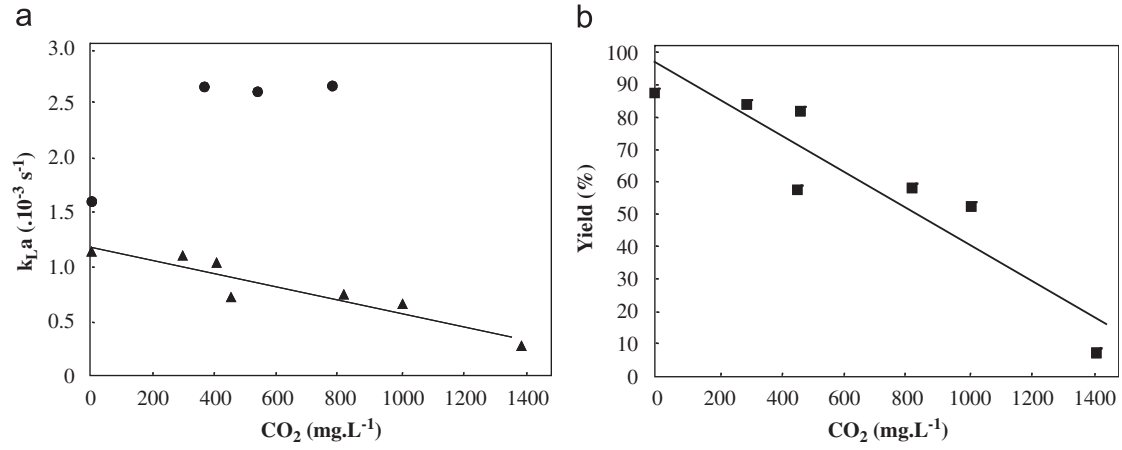

Fig. 7. (a) Values of K_La versus initial CO_2 concentration for absorption experiments (▲) and for desorption experiments (●) in a 20 L column—Oenodev distributor—synthetic solution—with synthetic air and nitrogen (D = 0.05 L/min). (b) Oxygen transfer yield for different initial CO_2 concentrations. Conditions as for Fig. 7a.

3.2.2. Carbon dioxide desorption during oxygen absorption

In Fig. 8a is presented an experiment, performed in the 20 L column saturated with CO_2 (corresponding to the last point of the decreasing curve in Fig. 7a), where desorption curve of CO_2 is shown in parallel with the absorption curve of oxygen. From these curves, very similar K_La values for oxygen and CO_2 were obtained (respectively 0.94×10^{-4} and $0.83 \times 10^{-4}\,s^{-1}$, see Fig. 8b). This could indicate that these cross transfers follow the same path, i.e., carbon dioxide does desorb via the oxygen bubbles, and that no parallel path, as nucleation for instance, is present.

3.3. Oxygenation of wine in presence of dissolved carbon dioxide

In Fig. 9a are presented the absorption curves performed with red wine, saturated or carbon dioxide free, with pure oxygen, in the 20 L column. The same trends, as in Section 3.2 are observed, i.e., a strong decrease in the transfer rates when carbon dioxide is present, which is reflected by much smaller values of the "apparent" K_La, decreasing from 1.10×10^{-3} to $1.29 \times 10^{-4}\,s^{-1}$, as seen on Fig. 9b. Nevertheless, note that, in the case of wine, the determination of K_La is likely to be affected by the oxygen consumption from certain constituents of the wine, as mentioned in the introduction. Specific conventional methods for determination of K_La, developed for fermentation processes, can be proposed to account for this phenomenon (Atkinson and Mavituna, 1983). In our case, for the sake of simplicity, oxygen consumption was assumed to be low enough to slightly affect the results.

Whatever the explanation around the K_La values, presence of dissolved carbon dioxide does result in a significant decrease of the transfer efficiency, where the oxygen transfer yield drops from 77%, when the wine is initially carbon dioxide free, to 9%, when it is initially carbon dioxide saturated.

3.4. Discussion

The dependence of K_La, during oxygen absorption or desorption experiments, in respect to initial dissolved carbon dioxide concentration, as seen in Figs. 6a or 7a, is quite puzzling, and the conventional modelling of the dynamic experiments used here may be questioned. Indeed, in these experiments, massive desorption of carbon dioxide into the bubbles of the oxygen or air stream, decreases significantly the partial pressure of oxygen in the bubble, and hence the saturation concentration C^*. Therefore, for absorption experiments, the values of K_La obtained from a model that assumes constant C^*, are "apparent K_La" values, because the actual difference of potential for transfer $(C^* - C)$ has been reduced. Indeed, the oxygen transfer rate does decrease when carbon dioxide is present, but the actual mass transfer conductance, which is represented by the parameter K_La, is probably not affected in the way readily deduced from the values of the "apparent K_La".

Conversely, in the case of desorption experiments, the oxygen dilution effect inside the bubble does not exist (oxygen partial pressure in the nitrogen bubbles is always close to zero, with or without CO_2), and, here, the observed flux increase can be attributed to an actual augmentation of the mass transfer conductance K_La.

An analysis of the situation, using simple physical considerations is proposed here, and reasoning using rough estimations will help assessing and comparing the quantitative influence of the different phenomena.

For instance, to estimate the decrease of the oxygen transfer driving force during absorption, i.e., the dilution effect, a simple calculation for the partial pressure of oxygen in the leaving gas stream can be done. Indeed, the carbon dioxide flux in the leaving gas stream is the desorbed carbon dioxide flux, and considering the beginning of the experiment, it could be obtained from the derivative of the desorption curve at $t = 0$, or more simply from:

$$\mathrm{Fs}_{CO_2} = (K_La)_{CO_2} C_{CO_{2i}} V_c \tag{4}$$

(note, it is similar to the maximum transferable flux, as defined in the Method section) where $C_{CO_{2i}}$ is the initial dissolved carbon dioxide concentration.

Similarly the transferred oxygen flux is

$$\mathrm{Ftr}_{O_2} = (K_La)_{O_2} C^* V_c. \tag{5}$$

So, the leaving oxygen flux Fs_{O_2} is equal to the oxygen flux entering via the gas flow Fe_{O_2} from which the oxygen transferred flux is subtracted:

$$\mathrm{Fs}_{O_2} = \mathrm{Fe}_{O_2} - \mathrm{Ftr}_{O_2}. \tag{6}$$

The oxygen flux entering via the gas flow, Fe_{O_2}, is given by

$$\mathrm{Fe}_{O_2} = D \frac{P_{O_2}}{P_T} \frac{1}{V_{\mathrm{mol}}} M_{O_2}. \tag{7}$$

When injection of pure oxygen is considered:

$$\mathrm{Fe}_{O_2} = D \frac{1}{V_{\mathrm{mol}}} M_{O_2}. \tag{8}$$

Now the molar fraction of oxygen in the leaving gas is given by

$$\mathrm{ys}_{O_2} = \frac{\mathrm{Fs}_{O_2}}{\mathrm{Fs}_{O_2} + \mathrm{Fs}_{CO_2}} = \frac{\mathrm{Fe}_{O_2} - \mathrm{Ftr}_{O_2}}{\mathrm{Fe}_{O_2} - \mathrm{Ftr}_{O_2} + \mathrm{Fs}_{O_2}}, \tag{9}$$

which gives

$$\mathrm{ys}_{O_2} = \frac{D \frac{1}{V_{\mathrm{mol}}} M_{O_2} - (K_La)_{O_2} C^* V_c}{D \frac{1}{V_{\mathrm{mol}}} M_{O_2} - (K_La)_{O_2} C^* V_c + (K_La)_{CO_2} C_{CO_{2i}} V_c}. \tag{10}$$

The partial pressure of oxygen in the leaving gas stream is then simply given by

$$\mathrm{Ps}_{O_2} = \mathrm{ys}_{O_2} P_T. \tag{11}$$

As already seen, in experiment of Fig. 8b, when $C_{CO_{2i}} = 1400\,\mathrm{mg/L}$, K_La values for CO_2 and O_2 are similar, and in the range of $10^{-4}\,s^{-1}$. So, using and $C^* = 41.1\,\mathrm{mg/L}$, the value

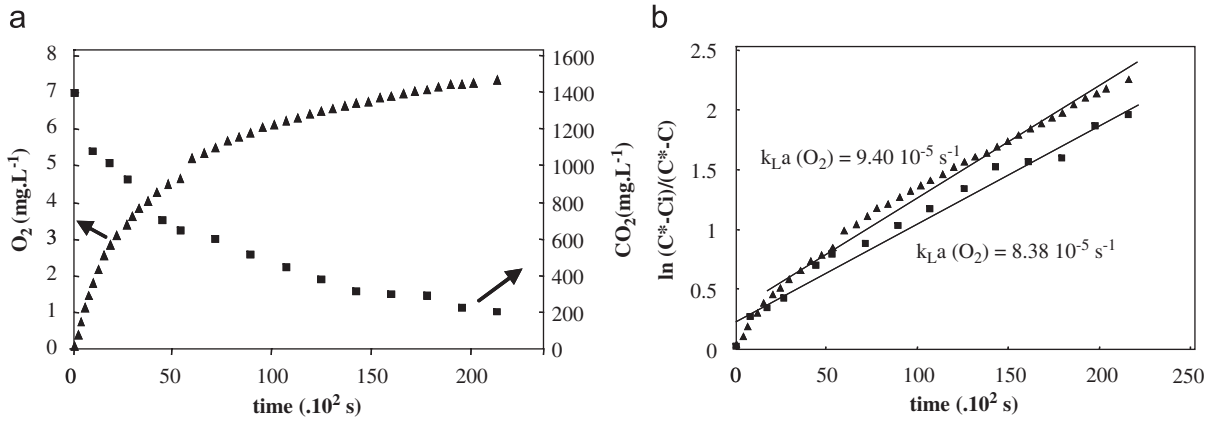

Fig. 8. (a) Simultaneous oxygen absorption curve (▲) and carbon dioxide desorption curve (■) in a 20 L column—œnodev distributor—synthetic solution—with synthetic air and nitrogen ($D = 0.05$ L/min), initial carbon dioxide concentration 1400 mg/L. (b) Simultaneous processed oxygen absorption curve (▲) and carbon dioxide desorption curve (■). Conditions as for Fig. 8a.

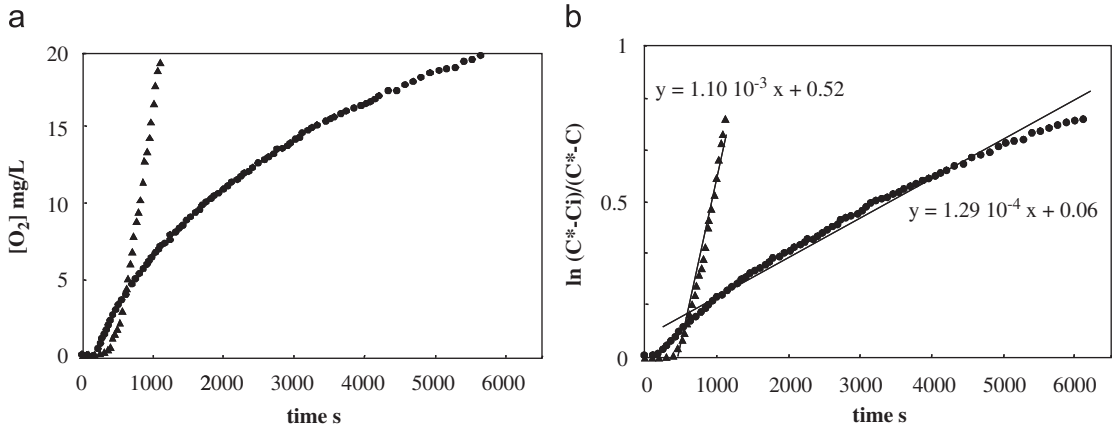

Fig. 9. (a) Absorption curves for oxygenation with pure oxygen in wine in a 20 L column, œnodev distributor, ($D = 0.05$ L/min), initially carbon dioxide free (▲), initially carbon dioxide saturated (•). (b) Values of K_La versus initial CO_2 concentration for absorption experiments in wine. Conditions as for Fig. 9a.

$ys_{O_2} = 0.26$ is obtained, that indicates that the partial pressure of oxygen in the leaving gas has been divided by 4, due to the transfer of CO_2. So, this means that the average driving force in the column (which is also related to the state of mixing in the gas and in the liquid) has been strongly reduced.

An attempt to explain the modification of the mass transfer conductance, K_La, is possible if effects upon the specific interfacial area, a, and those upon diffusional resistance, related to K_L, are uncoupled.

Because of the significant input of gaseous CO_2 into the bubble, the bubble diameter increases. For instance, in the case considered here, the four-fold-decrease of the oxygen partial pressure in the bubble is related to a four-fold increase of the bubble volume (because the transferred oxygen quantity is small in front of the transferred carbon dioxide quantity). This results in a $4^{1/3} = 1.58$-fold increase for the bubble diameter. This modification of the diameter induces two phenomena: (i) an increase of the bubble rising velocity, decreasing correlatively its residence time, (ii) an increase of the external area of every bubble. These two phenomena are antagonist in respect to the specific interfacial area, a, and it is expected that it will result in a weak modification of this latter, because the decrease of the bubble residence time is compensated by the increase of every bubble area. Indeed, the interfacial area inside the column is the sum of the areas of every bubble:

$$A = n_B \pi d_B^2, \tag{12}$$

where n_B is the number of bubbles in the column (the volume of which constitutes the hold-up). The bubble production rate (number of bubbles per second) at the distributor is given by

$$r_B = \frac{D}{(4/3)\pi d_{Bi}^3} \tag{13}$$

and assuming that it is the same, with or without CO_2 transfer. Therefore the number of bubbles in the column is

$$n_B = r_B t_{\text{res}}, \tag{14}$$

where t_{res} is the residence time of the bubbles in the column. A simple expression for t_{res} is

$$t_{\text{res}} = \frac{L}{v_B} \tag{15}$$

and the interfacial area, A, is then

$$A = r_B \frac{L}{v_B} \pi d_B^2. \quad (16)$$

In particular, if the bubble rising velocity is assumed to follow the Stokes' law (because of their small size, around 400 μm):

$$v_B = g d_B^2 \frac{\rho_L - \rho_G}{18\mu}, \quad (17)$$

the residence time is proportional to the inverse of the square of the diameter, while the bubble area increases proportionally with the square of their diameter. As expected, it results in an almost constant specific interfacial area, as deduced from Eq. (16).

So, we can now only suspect that the observed mass transfer flux augmentation is related to a modification of the liquid side mass transfer coefficient. This could be attributed, for instance to the increase of the bubble rising velocity, due to the bubble diameter increase with CO_2 desorption. Indeed, this velocity increase may affect positively the mass transfer coefficient.

With the light of these semi-quantitative considerations, it can be proposed that, for oxygen desorption experiment, the observed increase of the oxygen transfer flux is almost directly related to an increase of the mass transfer coefficient K_L. Conversely, in the case of absorption experiments, the antagonist dilution effect is the strongest, and results in a global decrease of the flux. Note that, in the case of absorption, because gaseous oxygen is leaving the bubble, its diameter increase is weaker than in the case of desorption, hence a weaker K_L enhancement.

This very simplified approach has the merit to justify the sense of variation of $K_L a$, and allows comparison of the quantitative influence of these phenomena.

4. Conclusion

This study has attempted to provide experiments likely to be representative of the mass transfer occurring during micro-oxygenation of wine in tanks. Their interpretation, using the conventional $K_L a$ analysis, has been presented and the validity of the approach has been discussed all along the text. Concerning the evolution of the transfer parameters when carbon dioxide is present, certain results remain insufficiently explained, and, especially, the influence of the direction of the concomitant oxygen and carbon dioxide fluxes is only partly understood. A deeper study, involving careful modelling of the coupled transfers occurring during these dynamic experiments for $K_L a$ determination, would certainly make it possible to uncouple the effects of an actual modification of the transfer conductance and those of the modification of the transfer driving force. Indeed, analysis and understanding of gas–liquid transfer proved to be not easy in the case of concomitant transfer of two gases, especially when they exhibit very different solubilities (remember CO_2 is almost 35 times more soluble than O_2). In this situation, the $K_L a$ approach, through dynamic experiments, must be interpreted with caution. Anyway, the undeniable result is that, during micro-oxygenation, oxygen transfer fluxes do decrease in presence of dissolved carbon dioxide. It was shown here that this affects directly the transfer yield, and this is of great importance in the actual operation of micro oxygenation of wines in tanks, because this could invalidate the hypothesis of total transfer that is always done.

Notation

A	specific interfacial area, m^2/m^3
C	instantaneous oxygen concentration, kg/m^3
C^*	oxygen saturation concentration, kg/m^3
d_B	bubble diameter, m
D	flow rate of the injected gas, m^3/s
Diff	diffusion coefficient, m^2/s
Fe	flux in the entering gas stream, kg/s
Fs	flux in the remaining gas stream, kg/s
Ftr	transferred flux, kg/s
g	gravity acceleration, m/s^2
H	Henry's constant, $Pa\,m^3/kg$
K_L	liquid mass transfer coefficient, m/s
$K_L a$	volumetric transfer coefficient, s^{-1}
L	height of liquid in the column, m
M	molar mass, kg/mol
n_B	bubble number
P	partial pressure, Pa
P_T	total pressure, Pa
r_B	bubble production rate, s^{-1}
t	time, s
v_B	bubble rising velocity, m/s
V_c	volume of the column, m^3
V_{mol}	molar volume of a perfect gas, m^3/mol
ys	molar fraction in the remaining gas stream
Y	oxygen transfer yield

Greek letters

μ	viscosity of the liquid, Pa s
ρ	volumic mass, kg/m^3

Subscripts

CO_2	referred to carbon dioxide
G	gas
i	initial
L	liquid
O_2	referred to oxygen

References

Artajona, J., Bobet, R., Marco, J., Sabat, F., Torres, M.A., Torres, M., 1990. Expérience d'hyperoxygénation au Penedes. Revue Française d'œnologie 124, 65–67.

Atkinson, B., Mavituna, F., 1983. Biochemical Engineering and Biotechnology Handbook. The Nature Press, New York, p. 737.

Blanck, G., 1990. Utilisation de l'hyperoxydation pour la valorisation des moûts de tailles en Champagne. Revue Française d'œnologie 124, 50–57.

Caputi, A., Ueda, M., Walter, P., Brown, T., 1970. Titrimetric determination of carbon dioxide in wine. American Journal of Enology and Viticulture 21, 140–144.

Castellari, M., Simonato, B., Tornielli, G.B., Spinelli, P., Ferrarini, R., 2004. Effects of different enological treatments on dissolved oxygen in wines. Italian Journal of Food Sciences 16, 387–396.

Dubourdieu, D., Lavigne, V., 1990. Incidence de l'hyperoxygénation sur la composition chimique et les qualités organoleptiques des vins blancs secs du bordelais. Revue Française d'œnologie 124, 58–61.

Fabre, S., 1994. Destination de l'oxygène consommé par le vin. Revue des Enologues 71, 23–26.

Farines, V., Hebrard, G., Poupot, C., Painmanakul, P., Mietton-Peuchot, M., 2005. Transfert d'oxygène dans les vins et les moûts. Récents Progrès en Génie des Procédés 92.

Getaz, J., Fabre, S., 1990. Mesure de l'absorption d'oxygène dans les moûts par la méthode D.B.O. Résultats et applications. Revue Française d'œnologie 124, 124.

Lafon Lafourcade, S., Larue, F., 1981. Viabilité des cellules en fin de fermentation alcoolique. Bulletin de la Société Française de Microbiologie Reims, 147–172.

Lopes, P., Saucier, C., Glories, Y., 2005. Nondestructive colorimetric method to determine the oxygen diffusion rate through closures used in winemaking. Journal of Agricultural and Food Chemistry 53, 6967–6973.

Meistermann, E., 1990. Hyperoxygénation des moûts—Essais réalises en Alsace. Revue Française d'œnologie 124, 62–64.

Moutounet, M., Mazauric, J.P., 2001. L'oxygène dissous dans les vins. Revue Française d'œnologie 186, 12–15.

Moutounet, M., Ducournau, P., Chassin, M., Lemaire, T., 1995. Appareillage d'apport d'oxygène aux vins—Son intérêt technologique. Enologie 95, Technique & Documentation Lavoisier, Paris, pp. 411–414.

Painmanakul, P., Loubiere, K., Hebrard, G., Mietton-Peuchot, M., Roustan, M., 2005. Effect of surfactants on liquid side mass transfer coefficient. Chemical Engineering Science 60 (22), 6480–6491.

Sablayrolles, J.M., 1990. Besoins en oxygène lors des fermentations œnologiques. Revue Française d'œnologie 124, 77–79.

Schneider, V., 1991. Comportement des vins obtenus par oxygénation des moûts blancs. Revue Française d'œnologie 130, 33–42.

Schneider, V., 1998. Must hyperoxidation: a review. American Journal of Enology and Viticulture 49 (1), 65–70.

Strehaiano, P., 1990. Oxygène et activité des levures. Revue des Enologues 124, 68–71.

Wild, G., LaraMarquez, A., Poncin, S., Midoux, N., 1994. Revue critique de techniques de détermination du coefficient volumique d'adsorption gaz-liquide $K_L \cdot a$ dans les réacteurs utilisés en biotechnologie. Récents Progrès en Génie des Procédés 34 (8), 109–114.